Materials Identification System for 200 liter/55 gallon Waste Drums using Computer Tomographic Techniques-17162

Joseph Harvill, Nuclear Waste Partnership LLC, Carlsbad, NM 88221, USA
Shelly Martinez, Nuclear Waste Partnership LLC, Carlsbad, NM 88221, USA
Daniel Schneberk, VJ Technologies Inc. 89 Carlough Road, Bohemia, NY 11716, USA.
Stephen Halliwell, VJ Technologies Inc. 89 Carlough Road, Bohemia, NY 11716, USA. shalliwell@vjt.com

ABSTRACT

In 2014 a thermal runaway event within a drum in-situ at the Waste Isolation Pilot Plant (WIPP) facility near Carlsbad, NM, resulted in the drum being breached and activity released. This emphasized the need for a better determination of drum contents and identification of material combinations and in-drum conditions. Enhanced characterization is required to identify and quantify the presence of absorbent materials, determine whether they are organic or inorganic, locate their position in the drum with respect to other materials, and quantify how much liquid is being held in the absorbent material.

As part of the waste characterization process to ensure compliance with the WIPP waste acceptance criteria, drums are currently inspected by Real Time Radioscopic (RTR) x-ray to identify prohibited items such as free liquids and un-punctured aerosol cans, but that technique cannot satisfy these newly identified requirements, and a new approach to non-destructive examination was required.

This approach complements the current RTR inspection with Cone-Beam Area Detector Computed Tomography (CT) scanning of the whole drum, followed by more-quantitative CT scanning of specific areas of concern, using a highly collimated Linear Detector Array. The density of representative waste drums required x-ray energies of up to 9MeV, which meant that sorting of materials by their photo-electric absorption is not viable as this occurs in the 80 - 180keV range. However, a notable characteristic of higher energy imaging in this context is the general correspondence between material density and total attenuation in the 1.5-4.0 MeV range due to Compton Scatter.

Development of the imaging chain, comprising the x-ray source and the detectors was critical to achieving the required system performance. Theoretical analysis of the energy spectra of the 9MeV beam, and filtration of the beam to remove the lower energies which cause beam hardening artifacts in the image was required. Theoretical evaluation of the required efficiency and image acquisition performance of area detectors and linear array detectors, was carried out to complete the selection of equipment. A system of density calibration rods was designed and, together with the selected equipment, was configured and used to acquire cone-beam CT data

and line-scan CT data by scanning a 55 gallon drum containing surrogate waste.

From the acquired data, CT reconstruction was performed and the basis of algorithms to identify materials were developed. Following this, a series of blind tests were done using a range of surrogate materials the contents of which were unknown to the system operators.

INTRODUCTION

X-Ray based CT inspection is a common Non-Destructive Evaluation technique employed in medical, industrial and security contexts. In particular, CT scanning of checked baggage is a demonstrated technology for detecting explosives and explosives-related contraband and is deployed in most commercial airports worldwide. We consider the structure of the scanning methods, detection algorithms, processing, and disposition of baggage to be a model for the inspection of WIPP waste drums, in spite of the differences between checked bags and waste drums. WIPP waste drums are much heavier with different constituent items. However, the recorded knowledge of the contents of the drum to the operator is more substantial compared to the scant information available on checked luggage. Also, direct ownership of the drums permits the use of certain measurement aids or at least some options for attaching imaging standards to the drums. Further, while timely inspections are to be preferred, WIPP drums are not connected to an impending flight, with the result that there are more options available for evaluating hard-to-inspect drums with multiple-techniques. Certain tiered-scanning options may be feasible which apply more scanning for suspicious drum contents, less for easy to characterize drums.

THEORY OF OPERATION: X-RAY BEAM AND DETECTOR CONSIDERATIONS

The lower-attenuating characteristics of checked luggage include some distinct advantages over waste drum inspection. Lower energy regimes, 80-180keV, intersect with documented multiple-energy techniques developed for materials identification, in particular estimation of Z-Effective [1], [2]. All of these techniques make use of the differing fall-off in photoelectric absorption, and the relative prominence of Compton scattering for materials of varying Atomic Number. Related to this, other techniques can identify materials by measuring the differing Backscatter behavior - again related to the proportion of Compton scattering across a range of materials [3]. For the higher attenuating WIPP waste drums much higher energies are necessary for adequate transmission signal. At these higher keV and MeV energies photoelectric absorption is not a significant component of total x-ray attenuation. For these higher energies, sorting materials by the proportion of photoelectric absorption is not viable.

A notable characteristic of higher energy imaging is the general correspondence between material density and total attenuation in the 1.5-4MeV range (dominated by Compton Scattering). The use of Hounsfield units [4] (or Modified Hounsfield units), where attenuation is measured as the ratio of total material attenuation to the attenuation of water (density=1) has interesting properties in this context. Figure 1 illustrates the ratio of attenuation to water for a number of low-Z and higher-Z materials for the 1.5-4MeV energy range. Notice the changes in attenuation are close to constant for lower-density materials, vary slightly over the 1.5-4MeV range for higher attenuating materials, and do not include sharp changes. Notice the lack of overlap between the attenuation ratios for different materials over the 1.5 to 4MeV range. Consequently, we consider a method for material identification using the attenuation ratio to water – or some other "Basis" material to be a tractable strategy. Second, even though the change in attenuation is gradual, it is significant, so additional precision can be obtained by measuring the effective energy for the scan – which will then track the change in attenuation. To do this we used a number of rods of materials with a range of different densities. The attenuation of each rod in the 1.5-4MeV region of interest is provided in figure 1.

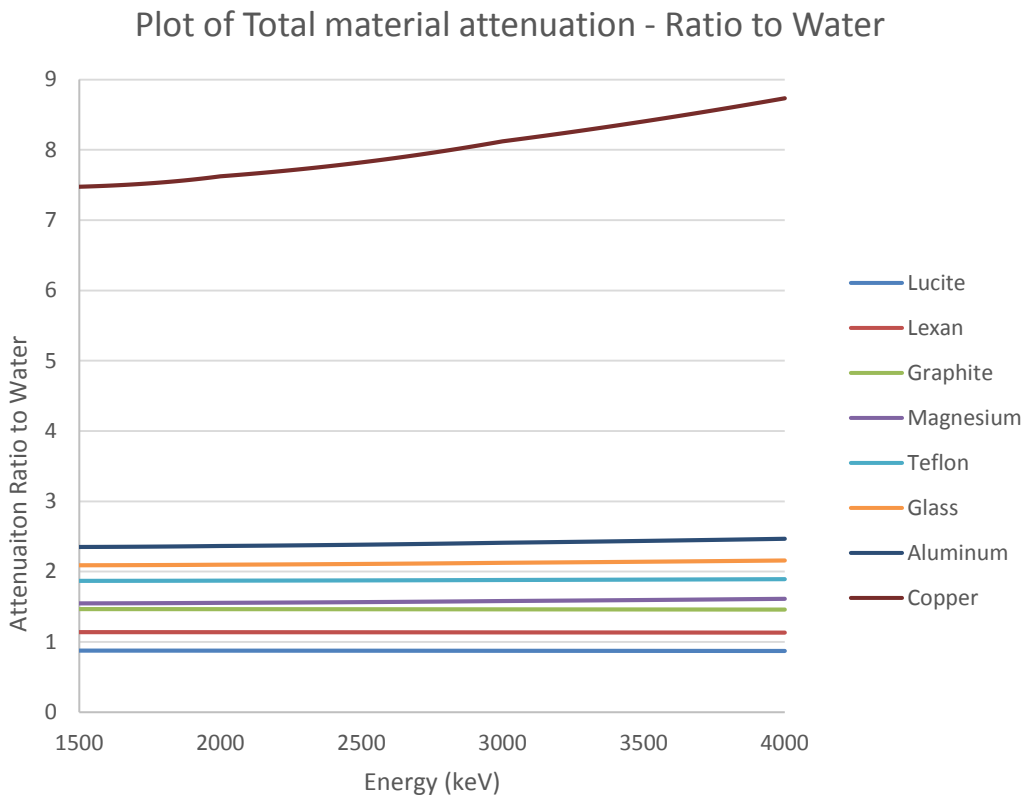

Figure 1 – Ratios of total attenuation to Water (Density=1) for different materials for the energy range of 1.5 to 4MeV

Unfiltered linear accelerator (LINAC) spectra include a substantial number of photons in the 500keV to 1MeV range, which can result in beam hardening artifacts when high-attenuating objects, like the waste drums, are scanned. Further, if the detector does not include substantial stopping power, the lower energy part of the source output is preferentially detected, resulting in a lower average energy used in the inspection. The result is an increase in artifacts, and the variation in measured attenuation can be due to source properties as well as the effect due to material differences. While it is possible to develop beam hardening corrections to adjust for this effect, these corrections can substantially increase noise in the reconstructed image.

Two methods of scanning drums were chosen. Both made use of the properties of scanning in the 2-4MeV range. It was chosen to scan with a 6MeV spectra and beam filtration of 12.5mm (½ inch) of Depleted Uranium (DU). The result was a spectrum with a higher overall average energy. Figure 2 shows a comparison using modeling techniques, of a 6MeV spectrum, and the same spectrum after transmission through the DU filter. Calculated from the numbers in the plot, the effect of the DU filter is to increase the average energy from 1.65MeV to 2.56MeV. The net result was less artifacts for both scanning methods used.

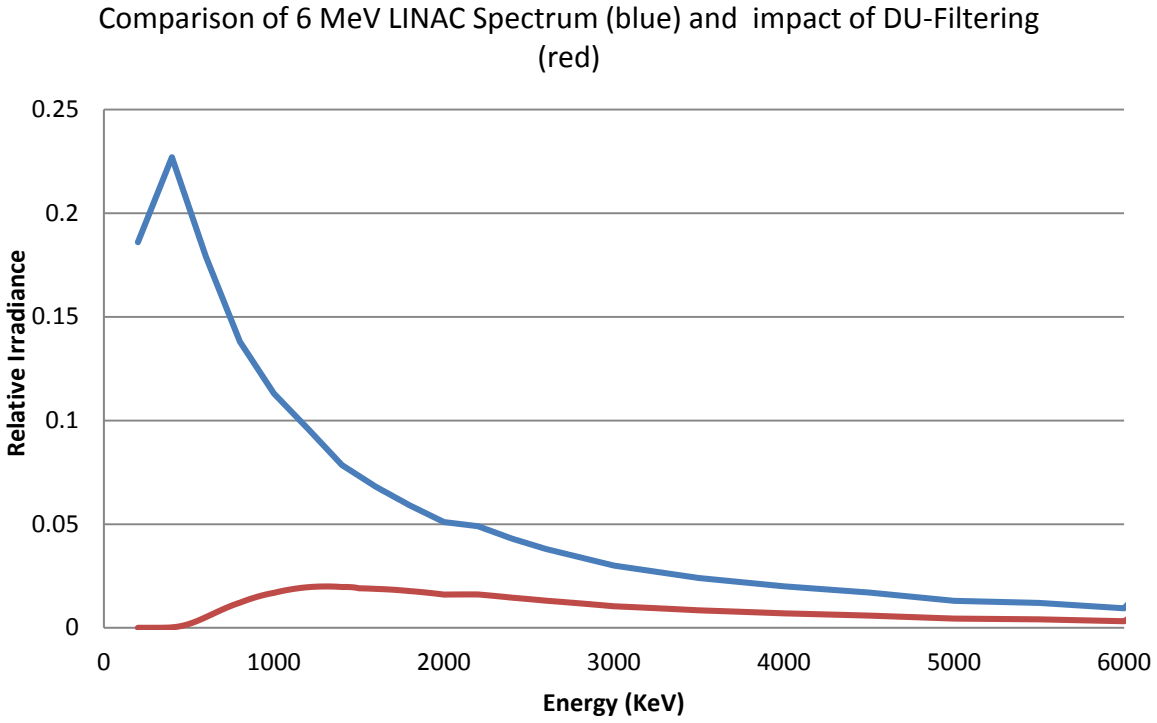

Figure 2 – Comparison of 6MeV LINAC spectrum, and impact of 12.5mm DU filtering

The stopping power of the detector and increased source collimation are additional factors impacting the distribution of artifacts in CT scans. The scintillator for the Area Detector used in Cone-Beam scanning, which is described in the next section, was 1mm of columnar Cesium Iodide (CsITl), a density of approximately 5.1 gm/cc. For the Linear Diode Array (LDA) detector scans, the scintillator was 1cm of Cadmium Tungstate (CdWO4) with a density of 7.9 gm/cc. Figure 3 shows a comparison of the DU filtered spectrum with the stopping power of the Cesium Iodide (blue) and the Cadmium Tungstate (red) accounted for in the respective plots. Notice the energy captured by the Cadmium Tungstate detector across the energy spectrum greater than the Cesium Iodide detector.

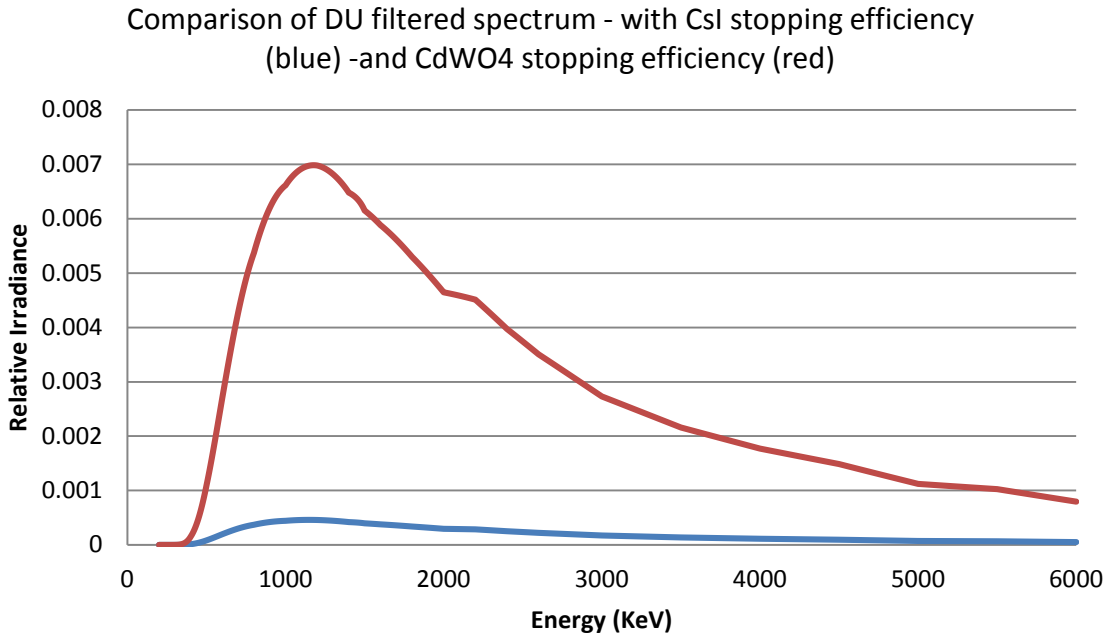

Figure 3 – Comparison of stopping power for 1mm CsI and 1 cm CdWO4 scintillators with a 6MeV DU filtered spectrum

THEORY OF OPERATION: COMPUTED TOMOGRAPHY SCANNING CONSIDERATIONS

An additional impact on the quantitative properties of CT scanning derives from the implementation of slit-collimation prior to the detector. Figure 4 illustrates the Area Detector scanning technique, whereas figure 5 illustrated the LDA scanning technique.

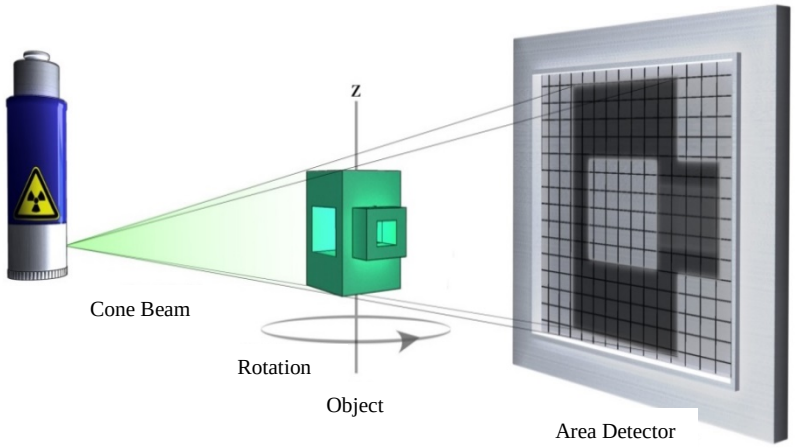

Figure 4 – Illustration of Area Detector (Cone-Beam) scanning

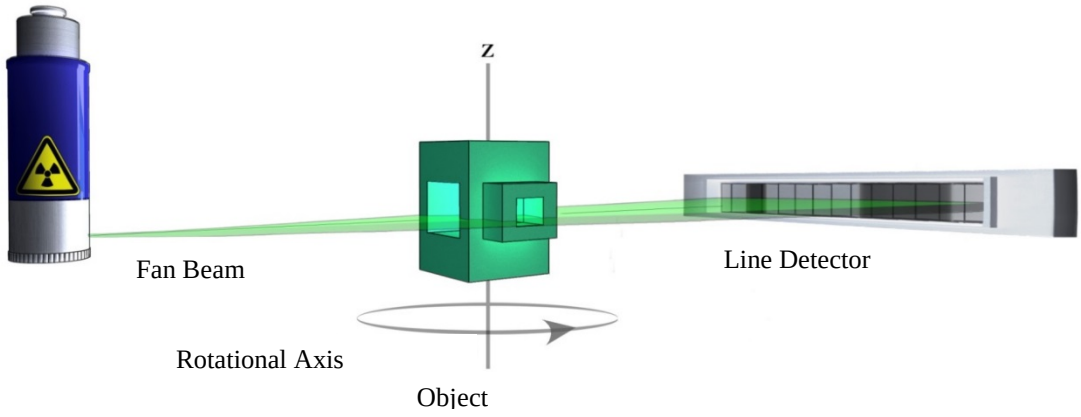

Figure 5 – Illustration of Slit collimated scanning with an LDA.

In general, independent of the detector the interaction of the source irradiance with the object generates an image in 3-space [5]. A detector element at a certain position and with a certain size will sample a specific part of this irradiance regardless of detector type. For any detector position, *d* (some 3D position on the other side of the object *O* from the x-ray beam), on a line *l* from the x-ray source *S(E)*, the detected x-ray photons intersecting this solid angle divide into different types as follows:

(1) $\Phi_T[S(E), O, d, l] = \Phi_P[S(E), O, d, l] + \Phi_S[S(E), O, d, l] + \Phi_{Rf}[S(E), O, d, l]$

(2) $\Phi_S[S(E), O, d, l] = \Phi_{Sbk}[S(E), d] + \Phi_{Sobj}[S(E) O, d, l]$

(3) $\Phi_{T0}[S(E), d, l] = \Phi_{P0}[S(E), d, l] + \Phi_{Sbk}[S(E), d]$

The schema above decomposes the photon output from an x-ray source *S(E),* for the solid angle subtended by detector area *d*, into primary irradiance, Φ_P, scattered irradiance Φ_S, and Φ_{Rf} refracted photons. The irradiance is from source *S*(E) (possibly polychromatic), undergoing x-ray interactions with object function O, along path *l* (a line from source to detector). Further there are two types of scattered photons; background scatter Φ_{Sbk}, and object scatter Φ_{Sobj}. It should be mentioned that Φ_{Sbk} can be decomposed further into scatter from the detector, from collimators and/or scatter from the fixtures/hardware within physical proximity to the detector, but determining this gets system dependent. Φ_{T0}, a measurement of the radiation field without the object, is fundamental to many x-ray measurements and is included here. Typically this measurement contains some background scattered photons from the supporting fixtures in the x-ray scanner or in the detection hardware, in addition to the primary photons launched by the x-ray source (in some instances the background signal can contain an image of the object container, if it is left in the field after the object is removed. One additional source of signal is the result of the digitization of the received signal $D(\Phi_T)$, and while the magnitude of this input depends upon the amount of signal to be digitized, it does not depend directly on the source-detector geometry or object, therefore, the subscripts have been left out.

CT scanning becomes more quantitative as the proportion of primary irradiance increases. This means that physical measures that can reduce the amount of scatter from the object, the detector, from the room, from behind the detector, will result in measured attenuation that tracks more with the “straight-line” average energy used in the inspection. The slit-collimated configuration implemented used for the LDA scanning eliminates substantial amounts of out-of-plane scatter, which is a significant source of detected signal at high energy. Further, the greater amount of stopping power for the LDA also reduces the amount of scatter from the intrinsic detector hardware (the metal backing from the detector and the detector case), and as indicated above, puts the effective energy used in the inspection in the 2-4MeV range.

Regardless of the type of scanning; cone-beam area-detector or slit-collimated LDA, the source irradiance from a LINAC is a spectrum. The source output can vary slightly from scan to scan, both in spectral content and in output. More importantly, the contents of the drum, with its own particular attenuation will change the effective energy transmitted in localized areas in the drum. Each change in energy will correspond to a

change in measured x-ray attenuation. To track this variation, and further assist in the identification of materials in waste drums a “jacket” of “calibration” rods was attached to the sides of the drum during scanning. This kind of scanning has also been referred to as the “Basis Materials” technique for performing materials identification. The jacket comprised a system of plastic fixtures for holding 9 rods of different materials which spanned the height of the drum, so the calibration rods are present in the CT reconstructed image for the entire contents of the waste drum. (See Figure 6). The design of the fixture will make the attachment of rods to the outside of a drum fast and easy, enabling rods to be changed without disturbing the contents of the drum. In this way, for each material in the drum, there is an array of calibration rods at that slice plane which saw the same spectra that inspected the material of interest.

INVESTIGATIONS USING “TRAINING DRUMS” WITH KNOWN CONTENTS

In order to investigate and evaluate the theory of operation a 55 gallon drum was filled with items representative of the waste stream that was in the problem drum at WIPP. The waste was placed into three plastic inner baskets to segregate the waste into three sections. Calibration rods were fitted to the outside of the drum. This was referrenced as the Training Drum, and was imaged using the two CT scanning methods previously described.

Figure 6 – Calibration jacket and rods attached to the outside of the Training Drum

The impact of the use of calibration rods can be shown in a review of the measured attenuation values obtained from a CT slice acquired with the Area Detector, with the contents identified. The slice is shown in Figure 7. In this scan the calibration rods consisted of Polycarbonate, Beeswax, Magnesium, polyethylene, glass, teflon and graphite (two of the locations were left empty). With this set of rods the material range for most accurate identification clusters was around materials in the 0.8-3 gm/cc range.

An additional feature for this “extended-CT” scan is the small artifact in the middle of the image. We used a 400mm x 400mm Area Detector to obtain this scan, and the minimum magnification we could obtain with this hardware resulted in a projected size of drum just “too-large” for our offset geometry. A plastic pipe was placed in the center of the drum. The anulus between the outside of the pipe and the side of the drum was then small enough to be projected onto the Area Detector. The “missing data” for the airspace in the middle of the pipe estimated using an “extended-CT” algorithm.

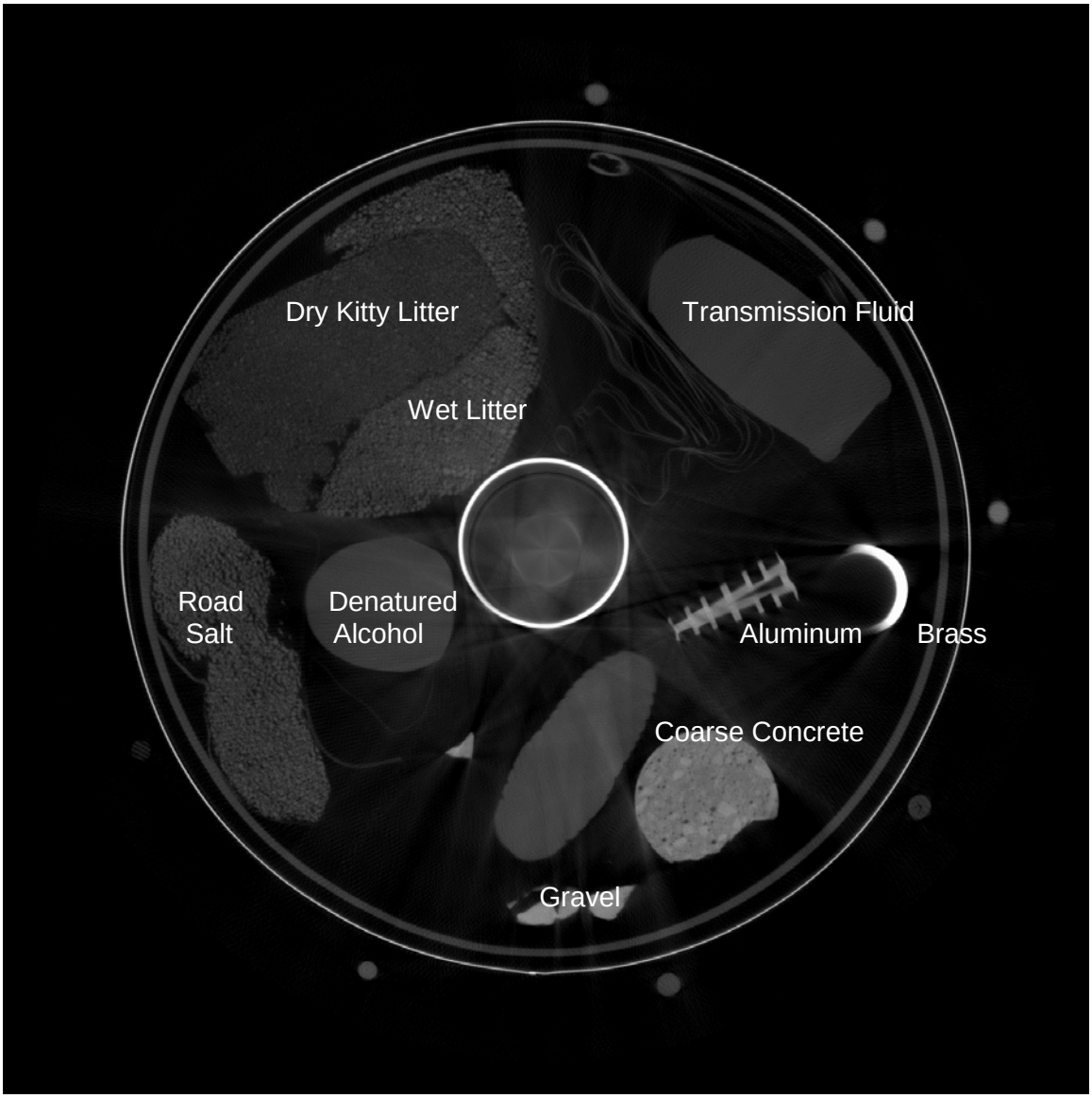

Figure 7 – CT slice from Cone-Beam CT system with low-mid-density calibration rods attached.

Alternatively, a different set of calibration rods with a different material range can be used. Figure 8 shows a slice acquired with the LDA configuration. The calibration rods for this scan included copper and tungsten, substantially increasing the range of material identification corresponding to this set of rods. In this case, the steel pipe in the middle measured less than the copper, and substantially less than the tungsten, making the identification of this material less ambiguous.

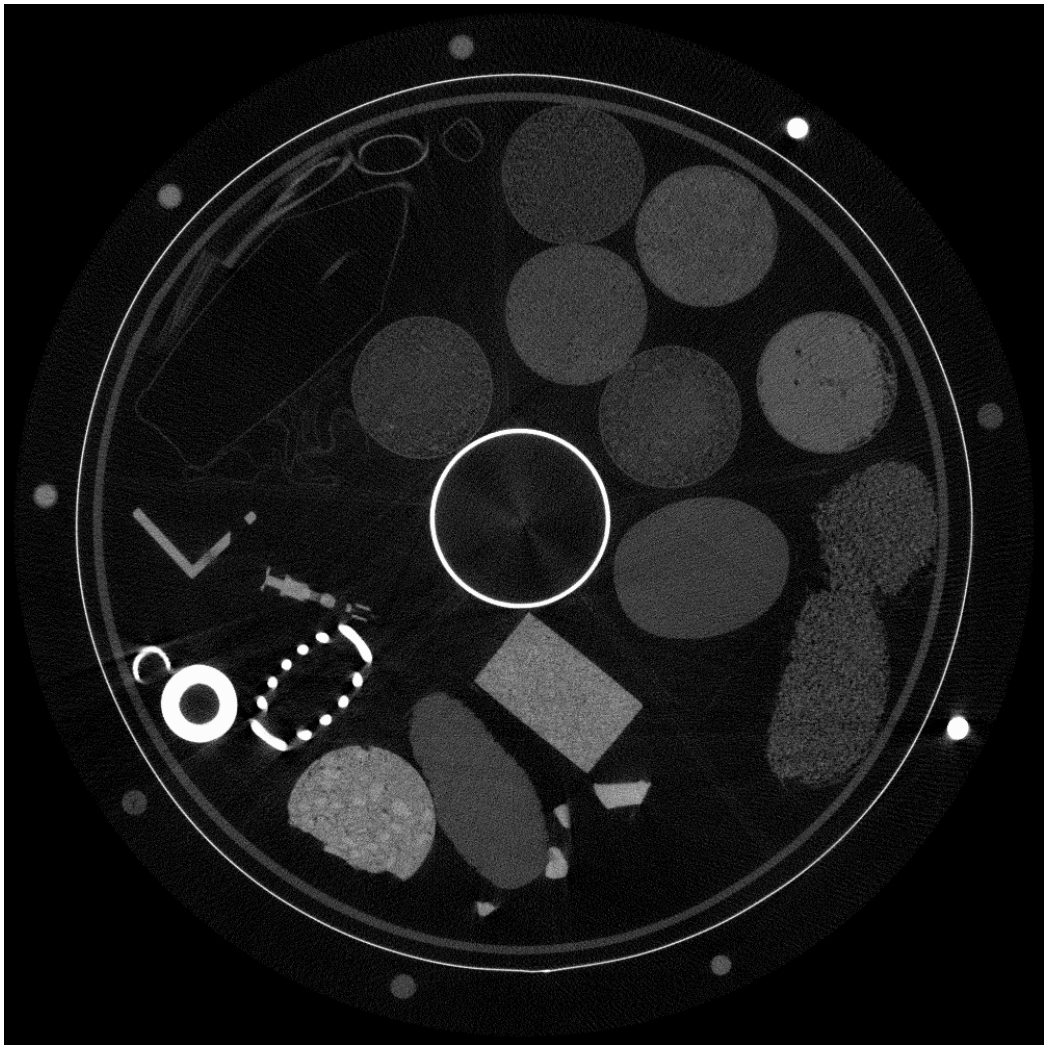

Figure 8 – CT slice from LDA based scanning with Copper and Tungsten in the set of rods

In all the scans of the test drum, the steel pipe in the middle is also used as a “calibration” material. However the purpose of the pipe was to assist in the “sectioning” of the test drum into regions, and for artifact reduction for the cone-beam scans. The different sections of the initial test drums was accomplished by inserting cardboard dividers at angular positons around the circumference of the central pipe. Also in Figure 8 is an array of different types of kitty litter, and kitty litter mixtures positioned in the 12 to 3 o’clock angular positions (more about these materials later).

The insertion of the calibration rods into every scan includes two implementation challenges. First, to process the acquired data to make the best use of the rods for a particular scan. Second, depending on the type of materials of interest to the inspection, to determine the best array of calibration rods for identifying items in a particular waste stream, and for

characterizing the items in the entire waste stream. Each waste stream may be better identified by a different array of calibration rods. Further, within a waste stream, the focus of the inspection may not be constant for every sub-population of drums, and as well may change depending specific issues with that waste, packed at that time.

In this first investigation, using the rods combines some semi-automated software and some requirements for the rods themselves. In particular, the densities of the rods need to be known with considerable certainty. Using the chemical formula and density we calculated the modified Hounsfield units corresponding to that particular known material. The density of each rod was calculated using accurately measured weight and volume data. Also, rods which had consistent uniformity down the length were chosen to ensure material composition and density was constant throughout the length of the rod – so the measurement of attenuation did not depend on the positional height of the object. Cracks in the rod, or gross porosity at some location along the length of the rod is problematic. Our Beeswax sample included a number of cracks and voids distributed down the height of the rod, making its use as a reference material haphazard.

Table 1 – Weights, Volume, Density & Modified Hounsfield of Calibration Rods

Material		**Weight**	**Length**	**Radius**	**Volume**	**Density**	**Modified Hounsfield Units (MHU)**
		gm	**cm**	**cm**	**cc**	**gm/cc**	**Total Atten/Atten-H2O (Avg 1.5-4 MeV)**
Wood (Fir		73	83.1	0.66	113.7663	0.6417	0.6127
Beeswax		90.5	83.1	0.63	103.6589	0.8731	0.9646
Polyethylene		170.5	83.9	0.82	177.3023	0.9616	0.9816
Polycarbonate		198	83.9	0.79	164.5663	1.2032	1.136
Carbon		182	83.1	0.63	103.6589	1.7558	1.464
Magnesium		184.5	82.8	0.63	103.2847	1.7863	1.576
Teflon		225.5	82.9	0.63	103.4095	2.1807	1.879
Glass		234	83.1	0.63	103.6589	2.2574	2.119
Titanium						4.5000	3.94
Copper		943	83.1	0.63	103.6589	9.0971	8.0067
Tungsten		2020.5	83.1	0.63	103.6589	19.4918	16.97

To enable the array of rods to be used, the rod material was automatically segmented from the rest of the scan, and for each image segment separate averages were calculated. The plotted values were used to estimate a function for converting the measured values to the known densities measured by other means. The resulting function was applied to every voxel in the CT scan. Once the CT volume was converted to modified Hounsfield units the values for the scans as representing the density-weighted attenuation of the materials could be interpreted. It should be mentioned here that there are different techniques for segmenting, estimating and applying the measured functional relationship between measured attenuation of the calibration rods and the voxels in the volume. These alternatives are currently being evaluated.
The CT volumetric images presented in figures 7 and 8 include more information than the voxel value used to scale to density. Notice that CT shows the complete 3D position of an object or material. Proximity of the different materials can be measured from CT scans. Secondly, the texture of the material is included in the voxel values in the CT scan. Texture can be defined as a distribution of particle sizes, as in the case with granular materials (the kitty litter and road salt in Figure 7). Or in the size of the regions of uniform intensity, as with the gravel pieces in the chunk of coarse concrete (also in Figure 7 and Figure 8). Notice with the concrete in figures 7 and 8 the same structure is imaged with either the Cone-Beam scanning or the LDA.

To gain some experience with different absorbents, a “test drum”was configured that included two different absorbents (two types of kitty litter). One was a “wheat” based organic kitty litter, the other was a “clay” based inorganic kitty litter. Each kitty litter was placed in a plastic bottle in the dry state, and in a separate bottle with water added. In addition, the organic and the inorganic kitty litters were mixed in a 50/50 ratio, and the mix placed in a bottle dry, and in a bottle with water added.

Figure 9 shows the same CT slice as in figure 7 but with the materials in bottles identified in the CT scan image. Table 2 includes some averages calculated from the different internal contents of the bottles obtained from the Area Detector scan and the LDA CT scan.

Table 2 – Average MHU calculated from Area Detector scan and LDA scan of Training Drum (with nominal calibration using rods including Copper and Tungsten)

Material	Area Detector	LDA Detector
Inorganic+Water	1.481707354	1.571089989
Dry Inorganic	1.189794746	1.053750832
Organic+Water	1.460297124	1.053750832
Dry Organic	0.933641275	0.863919895
50/50 Wet	1.438568119	1.303686542
50/50 Dry	1.120164991	0.989690140

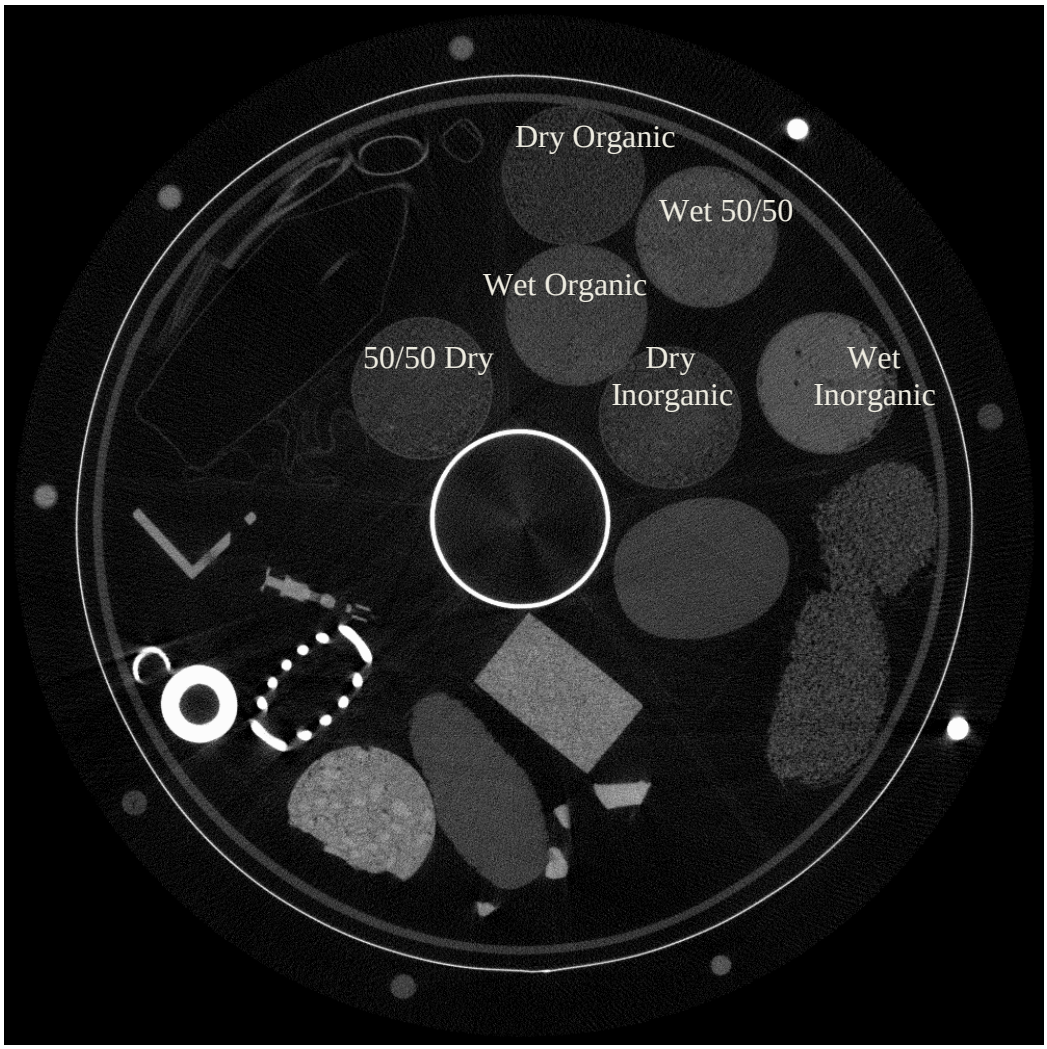

Figure 9 – CT slice with kitty litter samples acquired with LDA Scan at 6 MeV DU filtered

Also, from the training drum differentiation of the texture of the different absorbents – organic and inorganic, can be seen in the image For a variety of reasons the spatial resolution is a little better in the Area Detector scans.

Figure 10 shows a slice taken from the 3D volumetric data in the region where all 6 samples contain some material. Figure 11 shows vertical slices for each of the bottles to show the variation in measured attenuation down the height of the material in the bottles. It is important to note the change in attenuation as more liquid is absorbed into the material. Also, notice that for the granular materials, the vertical packing makes a small difference to the attenuation. That is, the cluster of absorbent for the dry samples includes some variation in attenuation with height. For the dry samples, and in the dry section of the bottles containing water, notice the particle size can be identified in the texture. It appears for these samples the particle size of the clay kitty litter is larger than the particle size for the wheat or organic kitty litter.

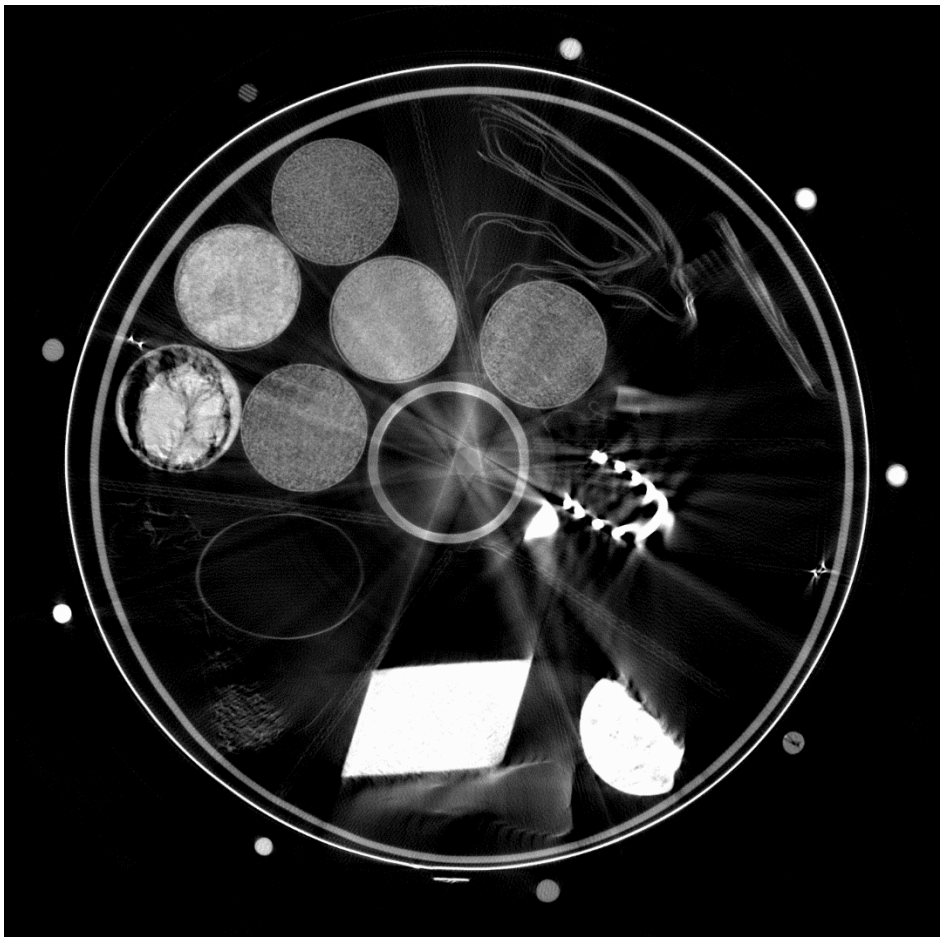

Figure 10 – Cross-sectional slice from cone-beam volumetric data which shows difference in texture between Organic and Inorganic kitty litter

Figure 11 – 4 Vertical slices through 3D cone-beam volumetric data showing (from top to bottom): Dry Organic, Wet 50/50 & Wet Organic, Wet 50/50 & Wet Organic & Dry 50/50 and Wet Inorganic & Dry Inorganic.

From the scans of the training drum including the 6 samples of kitty litter: Inorganic Dry, Inorganic Wet, Organic Dry, Organic Wet, 50/50 Dry and 50/50 wet the following conclusions were made:

1) The attenuation (density) value of this organic kitty litter is lower than the density of this inorganic kitty litter.
2) The particle size for the inorganic kitty litter is larger than the organic kitty litter.
3) Vertical packing for the two kitty litter's appears to be different, as is the variation in absorptance, as measured by the change in attenuation down the height of the bottles containing the samples.
4) As an aside, the nominal calculated values for the Kitty Litter samples varies somewhat with the selection of calibration rods. It will be important to select the most appropriate array of calibration rods prior to scanning more drums.

It was considered that these properties would be part of the signature for each of these materials and the information would be used to identify materials from both the Cone-Beam scanning and the slit-collimated scans with the LDA. Also, the trend in the differences between the materials; organic equates to smaller particle size, lower density and more variation in absorptance as compared to the inorganic absorbent materials was used in the next stage to test the previously described rationale for materials identification.

TESTING OF MATERIALS IDENTIFICATION FUNCTION USING "BLIND" TEST DRUMS

Four 55 gallon drums were packed by the Nuclear Waste Partnership team with a range of waste materials that were representative of the problem waste stream. The types of waste and configuration within these "Blind Test" drums was not known to the test team.

The four Blind Test drums were each scanned with the Area Detector, Cone-Beam scanner using the 6 MeV DU filtered spectrum. Due to constraints related to the available CT scanning equipment, we employed the same "extended CT" algorithms for the cone-beam CT acquisition. The minimum magnification for the Cone-Beam scans was 1.23 (4368.0mm source-to-detector distance and 3556.0mm source-to-object distance). At these distances the 400mm x 400mm Area Detector did not quite span the ½ projected area of the drum plus the calibration rods. As a result, for half-

scan image acquisition, also known as Off-set scanning [6] (see Figure 12) we have a “dead region” in the middle of the drum. In this region we effectively have no data on the object. Again, to mitigate the artifacts resulting from this geometry we placed a PVC pipe in the center of the drum, and intentionally left the region empty.

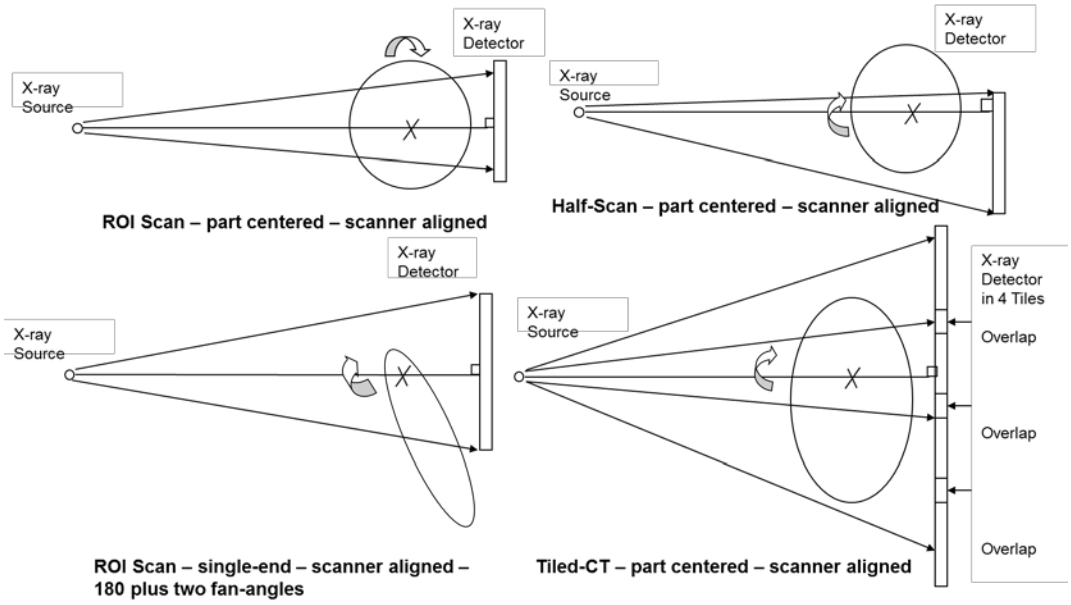

Figure 12 – Assorted scan geometries for objects larger than the scanning envelope. The half-scan, or offset-scan geometry is illustrated in the upper right corner of the figure.

The acquired data was processed to reconstruct voxels in the 0.5mm range. The Cone-Beam scanning included 800 views over 360 degrees. The Area Detector has a pixel size of 0.2mm, and at this magnification, the reconstructed voxel size would be 0.1628mm. For a number of reasons we elected to resample the acquired radiographs into 0.6 mm pixels, and reconstruct into 0.4884 mm voxels. First, the spot size of the LINAC through the DU filter cannot support this resolution. Second, it is considered that voxels in the 0.5mm range were sufficient to identify objects and locations for further scanning with the LDA if necessary. It is important to note that we could scan at a higher resolution, but to reduce Moire artifacts we would need to acquire more views, which requires more time.

For Cone-Beam CT scanning the input data are radiographs. In many cases these data are the same digital radiographs displayed for the inspectors performing Real Time inspections. While the CT input data is acquired in a sequence without operator intervention, this does not prevent the use of the rotational views as inspection data. Viewing this data can provide insights into locations and regions of interest in the drum, and can direct the evaluation of the CT volumetric data.

3D CT volumetric data provides great detail on the state of the drum contents. A CT volumetric data is a "voxelized" measurement of the x-ray attenuation of the object. At each 3D position the measured voxel reflects the attenuation of the materials contained in that volume-element, according to the effective energy of the inspection in that region. As such the data set includes the identification of edges and boundaries, as well as material changes in a particular matrix. Unlike radiography, CT can present an unambiguous image of the components in the object, in this case a waste drum. At the same time, there are limitations on the kinds of claims and measurements possible from CT reconstructed data sets. The combined properties of the particular scan result in a certain contrastive and spatial performance, which will define the limits for measuring differences in intensity as well as measuring the size of features. We have relied on techniques described in ASTM 1441 to support the inspection claims presented below.

Substantively, this review of the 3D data focused on the identification of items in the drums. Absorbent materials were to be identified, and an initial comparison made with the acquired data from the training drum. The 3D volumetric data was used to estimate a volume of each identified absorbent material. It was anticipated that there could be more than one absorbent material in the different drum loads. It was decided to report as many estimated volumes of material for the different materials identified since these numbers can always be aggregated into a "total absorbent" measurement if need be. Locations were picked from these regions for the more quantitative LDA scanning to provide more data on the identity of absorbents. Both the texture data obtained from the Cone-Beam scanning and the voxel measurements from the LDA scanning was used to determine the organic/inorganic status of the material.

It should be mentioned here that we are not satisfied with our treatment of "pore-spaces" between absorbent particles, and how absorbent materials change with the introduction of liquid. Consider the analysis presented here to be our first approximation to this task. A next phase of this effort focuses on scanning the different absorbent types with varying amounts of liquid.

Based on the acceptable knowledge of the waste stream that was simulated, an array of calibration rods that were oriented to the lower-Z non-metallic end of the material spectrum was chosen. The array of rods used were: Wood, Beeswax, Polyethylene, Polycarbonate, Graphite, Teflon, Glass, and Titanium. The same rods were used for all of the scans: the training drum scan, the Cone-Beam scans of the drums, and the LDA scans of the drums.

As mentioned above we used the values from the Basis-Rods to convert the voxels in the drum to Modified Hounsfield Units (MHU). Three issues arose in the course of our analysis. The Beeswax developed cracks over time and we ended up excluding this material from the functions used to convert the voxel values of items to MHU. Also, the Fir (wood) rod included anomalies related

to the "tree rings" in the material. Further, the Copper rod resulted in too many local scatter streaks. As a result the MHU values presented here were calculated using the Polyethylene, Polycarbonate, Carbon, Magnesium, Teflon, Glass and Titanium rods.

SUMMARY OF RESULTS OF SCANNING OF THE BLIND TEST DRUMS

The contents of each drum, as determined from both scanning techniques, are listed in the following tables, 3 through 6. Figures 13 through 15 show sample images to illustrate the resulting information.

Table 3 - Summary Table of Contents for Drum #1

Item Name	Position	Material	Reviewer Decisions & Notes
Metal Bracket	Upper Section	Steel	Picked Steel MHU > Titanium
Slab of Wood	Spans upper and Lower Section	Wood	
Metal Plate	Mid-Lower Section	Steel	MHU> Titanium
3 bottles containing different substance Bottle #1 Bottle #2 Bottle #3	Bottles 1 and 2 are at bottom of load with Absorbent Bag #3 on top. Bottom of Load Bottom of Load Encased in Absorbent Bag #3	 Plastic Plastic Glass	 Bottle #1 – may contain liquid MHU –> 1.2 Bottle #2 – contains clay or soil MHU -> 1.4 – inner contents, and 1.5-1.6 for outer bottle Bottle #3 – may contain liquid and has granular texture – could be absorbent – MHU -> 1-1.2
Metal Slug	Mid-Upper Section	Aluminum	MHU = 2.4-2.5 - Aluminum
Low Density Masonry Brick	Lower Section underneath Bag #3	Gravel pieces in matrix	MHU = 1.2 for matrix, 2.2-2.4 for clusters in Brick (Gravel)
Metal Staples	Mid-Lower Section	Steel	MHU > Titanium
Plastic Bags	Various surrounding different items		Material is Thin – so with Partial volume – MHU-> 0.6-0.8
4 Bags Absorbent		Absorbent	

Bag #1 Bag #2	Bottom close to Plastic Container Bottom Close to Wood and Metal Slug	Organic Absorbent Inorganic	Grain Size small and MHU-> 0.78-0.82 (Volume 491.4 cc.) Grain Size Medium and MHU->0.86-0.88 (Volume 433.9832cc.)

Table 4 - Summary Table of Contents for Drum #2

Item Name	**Position**	**Material**	**Reviewer Decisions & Notes**
Plastic Bags	Upper section and throughout	Plastic	Material is Thin – so with Partial volume – MHU-> 0.6-0.8
Tall Cuboid (Brick) of Material	Spans most of the vertical distance of the load	Lightweight porous material	Material is low attenuation – MHU -> 0.9-1.0 – 114mm x 64 mm x 230 mm -> 1680 cc Might be filter material
Metal Bracket	Upper Section	Steel/Brass	MHU-> Titanium
Threaded Metal Pipe	Upper Section	Steel/Brass	MHU> Titanium
Metal Cylinder w' Hole in Middle	Upper Section	Steel/Brass	MHU> Titanium
Metal Pipe with machined-closed end	Upper to middle section with substantial section embedded in absorbent	Steel/Brass	MHU>Titanium
Metal Container – in shape of Can	Lower Section	Metal Alloy	MHU -> 3.5-4 – MHU will be lower with partial volume – but this material lower than other metal parts – could be Steel/Alloy
Plastic Bracket	Upper Section	Plastic	MHU -> 0.8-1.2 - measurements likely low due to partial volume
Batteries (9)	Mid to Lower section	Hi-Z pole in center, layered metal surrounds	Metal Outer layer measures about 4-5 MHU – inner central rod measures as high as 8-9 MHU
Bag or Blob of Material	Mid-Upper through Lower Section	Absorbent or Filter	MHU -> 0.72-0.78 Almost no observable texture (Volume 928cc.)

		Material Organic	
Large Bag of Absorbent	Mid to Bottom of Load	Absorbent Inorganic	Grain Size Medium to large and MHU->0.82-0.92 Considerable variation which does not appear to be due to packing – likely due to absorbed material (absorbent is partially wet) (Volume 4,926cc.)

Table 5 - Summary Table of Contents for Drum #3

Item Name	**Position**	**Material**	**Reviewer Decisions & Notes**
Plastic Bags	Upper section and throughout	Plastic	Material is Thin – so with Partial volume – MHU-> 0.6-0.8
Plastic Packing Material	Upper Section and throughout	Plastic	Material is Thin – so with Partial volume – MHU-> 0.6-0.8
Paint Can of Material	Middle to Bottom	Lightweight material with little if any texture Organic.	Material in can is low attenuation and minimal texture MHU 0.6-0.8 (Volume 2,440cc.)
Plastic Bottle filled with Liquid and Absorbent	Middle-Bottom	Plastic outer with Absorbent and Liquid Organic	Section at top is granular and section at bottom indicates substantial liquid has been absorbed – particles are large with MHU in the 0.7-0.9 range for wet material. (Volume 2,243cc.)
Rubber/Plastic Hoses (3)	Spans the height of the load	Rubber/Plastic	MHU-1.2-1.4 range
Metal End Hammer with Wood Handle	Middle to Lower Section	Wood handle and Heavy Metal Head	MHU> Titanium
High-Z Flexible Metal Sheet	Upper to middle section	Lead Sheet	MHU>Titanium
Sponge Underneath Paint Can	Upper Section	Cellulose	MHU -> 0.6-0.8 range

Table 6 - Summary Table of Contents for Drum #4

Item Name	**Position**	**Material**	**Reviewer Decisions & Notes**
Plastic Bags	Upper section and throughout	Plastic	Material is Thin – so with Partial volume – MHU-> 0.6-0.8
Plastic Packing Material	Upper Section and throughout	Plastic	Material is Thin – so with Partial volume – MHU-> 0.6-0.8
Paint Spray Bottle (Empty)	Upper section	Plastic	Plastic material with different materials in the trigger section of the bottle
Plastic Box with low attenuating Insulation	Upper Section to middle	Box is plastic with rags or something layered inside	MHU of box is 1 or so – layered contents is less attenuating in the 0.6 range
U-Shaped Filter Material	Upper Section	Could be insulation or Filter Material	MHU 1.1-1.2
Plastic Container with Absorbent	Upper section	Absorbent wet and dry Organic	MHU 0.6-0.8 Dry – 0.8-1.1 Wet (Volume 480cc.)
Stack of Paper – could be stack of Paper towels folded	Upper Section	Two Stacks – one is ruffled the other is orderly	MHU about 0.9
Plastic Scraper – without Blade	Upper section	Plastic with Plastic Handle	Scraper does not appear to have a blade in it – right in Paper stack
Flexible Plastic Container w Water	Middle Section	Container is flexible with a nozzle at the top	Plastic flexible container includes fluid that has an MHU close to 1
Wood Slab	Middle to Lower	Wood – 2x4	MHU – 0.5-0.8
Glass Containers (2) w' Liquid	Middle to Lower Section	Glass containers with liquid	Outer material has MNU close to 2 – liquid is in the 1.2 range – so has the density of say glycerin
Flexible Thin Metal Plate – Bent into 2 layers	Upper to Lower Section	Metal – Likely Aluminum	MHU is about 1.8 to 2 – but expect partial volume effects
Plastic Bottle with Water	Middle Section	Plastic	Bottle contains a little liquid with MHU < 1.0

Plastic Tube with connector	Middle	Plastic	MHU- 1.0-1.2 range- Glass tube connected to tube – MHU - 2
Paper File Folders	Upper to Middle	Paper	MHU < 1.0
Absorbent Bag	Middle to Lower	Absorbent Organic	Absorbent includes regional variation resembling the wet/dry differences in training drum (Volume 2,027cc.)
Glass Container with Handle	Upper-Middle	Glass	Glass material (could be light Aluminum MHU-2.1-2.3 – shaped like Glass Measuring Cup (multi-cup size)
Rubber/Plastic Hoses (3)	Spans the height of the load	Rubber/Plastic	MHU-1.2-1.4 range
Absorbent with both wet and dry sections	Middle to Lower Section	Granular Absorbent	MHU> Titanium
Metal Slug or Cylinder of Metal	Lower Section	Aluminum	MHU > 2.3-2.6
Keyhole Saw	Lower Section – embedded in wet/dry absorbent	Wood Handle Metal Blade	MHU>Titanium
Rubber Plastic Hose	Lower Section	Rubber/Plastic	MHU -> 0.6-0.8 range
Coil of Small plastic tubing	Lower Section close to bottom	Rubber/Plastic	MHU > 1.0-1.4
Plastic Bags/Packing	Lower Section close to bottom	Plastic	MHU > 0.6-0.8
Metal Spigot	Lower Section close to bottom	Metal – Steel or Copper	MHU>Titanium
Metal Hammer with Wood Handle	Lower section close to bottom	Metal Head and Wood handle	MHU>Titanium
2 Metal Plates	At Bottom	Metal – likely Steel	MHU >= Titanium

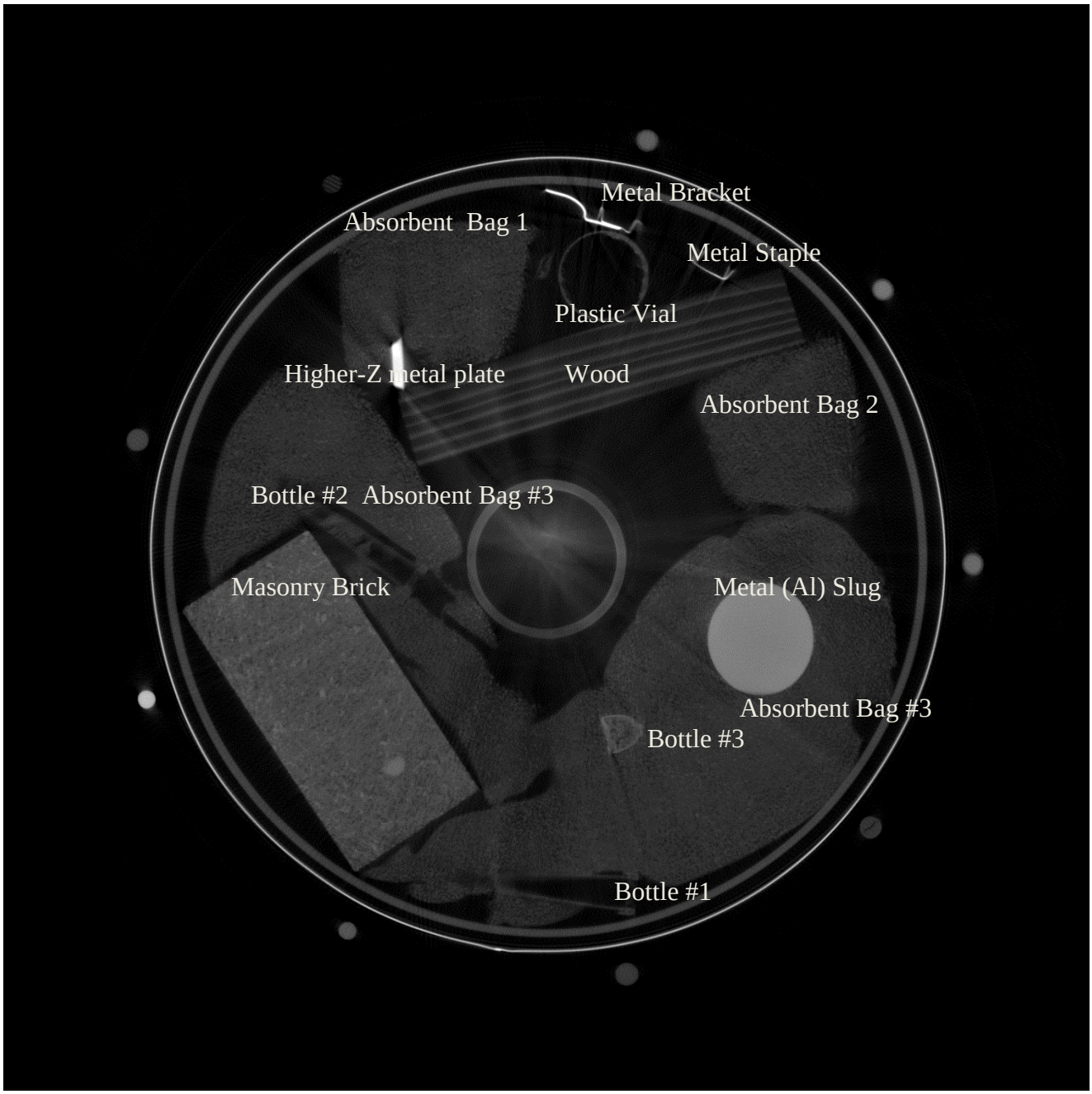

Figure 13 – Blind Drum #1, Cone Beam scan of Cross-sectional CT slice showing 3rd bottle, metal staples, and Higher-Z metal plate.

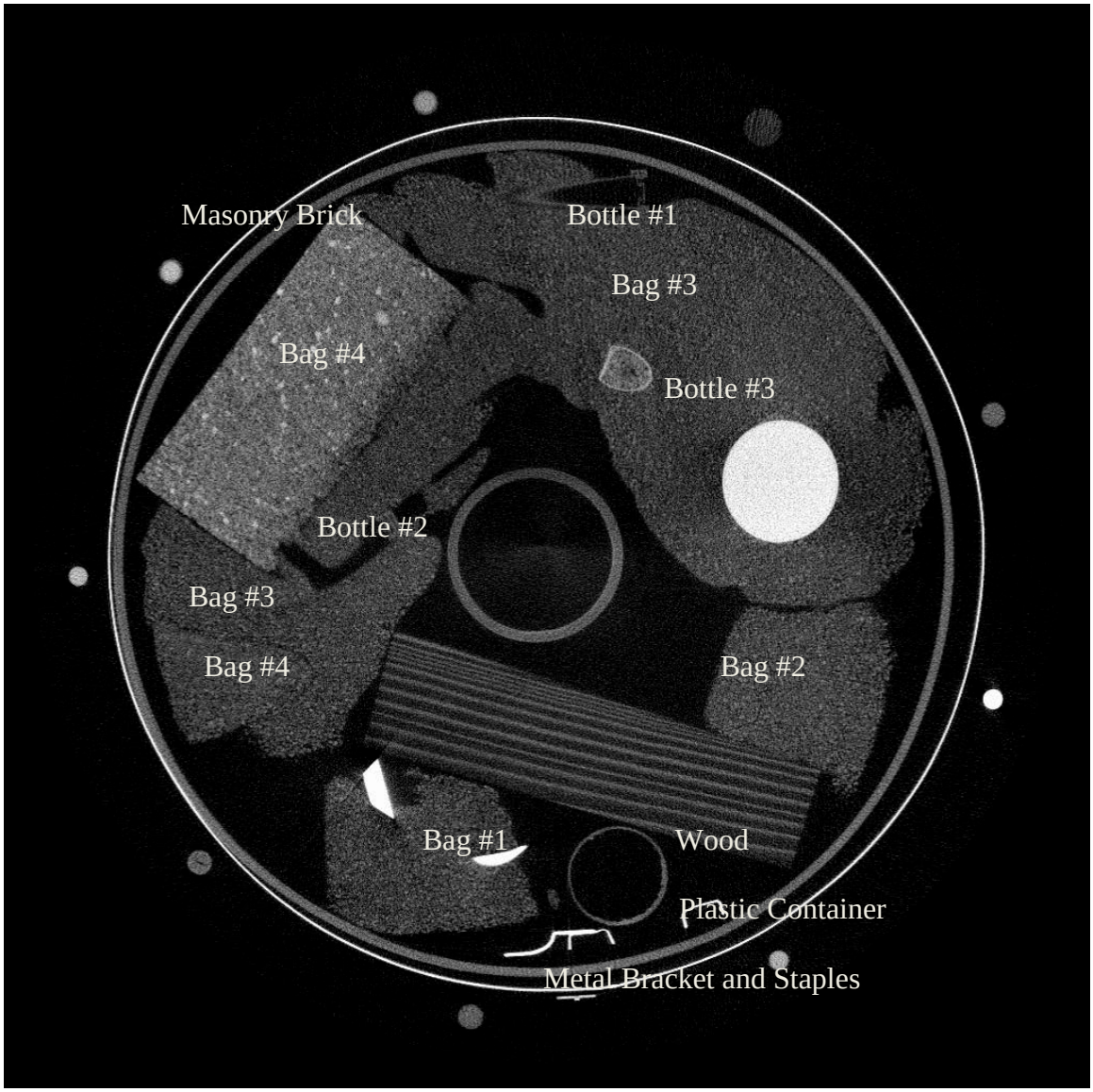

Figure 14 – Cross-sectional LDA slice of Blind Drum #1.

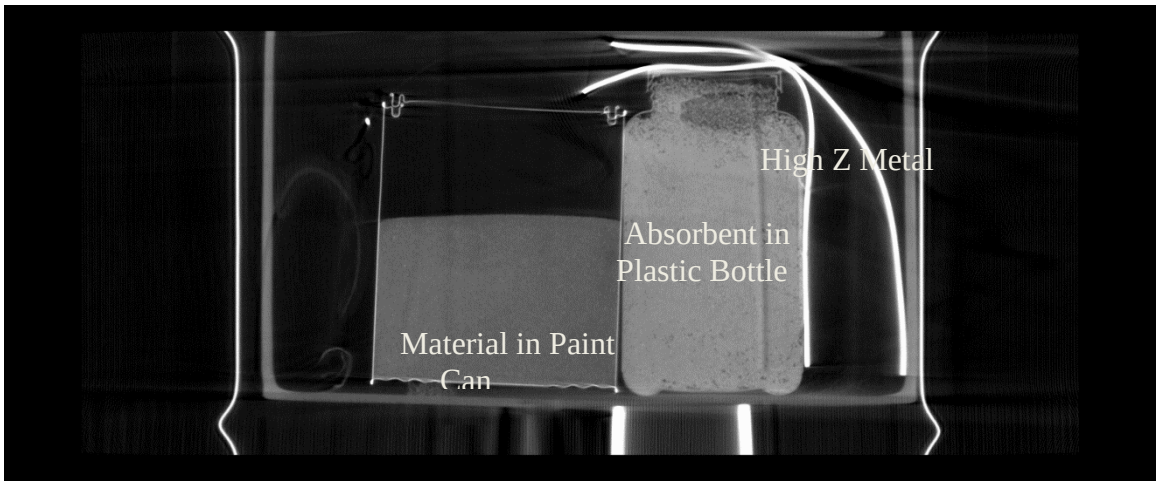

Figure 15 – Vertical slice from Drum #3

CONCLUSIONS

The scanning performed on the four Blind Test drums showed the following:

- The Flat panel Cone Beam CT included enough detail to identify many items, but included some streak/beam hardening artifacts that made materials identification difficult.
- The LDA scans included images with less artifacts and are more quantitative, but with less resolution.
- Identifying absorbents is complicated by the changes in packing-density for different configurations of absorbents: loosely packed in a bag, placed in a cup or underneath an item with substantial weight. This variation in packing properties impacts the measurement of attenuation.
- More “training” data beyond what was acquired from the single training drum will be required, to further identify the difference in the wet/dry regions in the absorbents in the Blind Test drums varying more than desired from the differences in the training drum materials.
- Some extra variability in results was exhibited in the scan of Drum #3, when the LINAC was not operating with consistent output. This was corrected for subsequent scans, but this identified the need to include some extra checks on the LINAC output to achieve better quantitative scanning.

NEXT STEPS

- Scan all the possible absorbents, with controlled amounts of liquid introduced to enable a look at partially absorbed and fully absorbed materials.
- Identify the likely liquids that will be contained by the absorbents, and scan the different wet/dry conditions.
- Evaluate the different packing schemes for loosely packed absorbents.

- Scan a set of drums based on total attenuation in order to develop methods for calculating more precise MHU values for the different amounts of attenuation in drums.
- Find new basis materials in the low-density low-attenuation range as replacements for the Beeswax and the Fir Rods. These new materials should be chosen to make automated segmentation and calculation of mean or median values more stable.

IMPORTANCE OF THIS WORK

The ability to identify problematic materials within a drum or waste package, by non-destructive examination, eliminates the need for complex and expensive equipment to open and remotely handle the waste, avoids potential hazards and risk of personnel dose uptake, and does not increase the volume of waste caused by repackaging of materials after examination and the decontamination or disposal of equipment used.

REFERENCES

[1] R.E. Alvarez and A. Macovski, Energy selective reconstructions in x-ray computed tomography, *Phys Med Biol* 21(5) (1976), 733–744.
[2] Ying, Z., Naidu, R. and Crawford, C.R., Dual energy computed tomography for explosive detection, *J X-ray Sci Technol*, 14-4, 235-256, 2006.
[3] Glover, Jack L., Hudson Lawrence T., A method for organic/inorganic differentiation using an x-ray forward/backscatter personnel scanner, *X-Ray Spectrometry* 2013, 42 531-536.
[4] Hounsfield, G.N., Computerised transverse axial scanning (tomography) I. Description of system, *Brit J Radiol* 46, 1016-1022, 1973.
[5] X-Ray Imaging: Fundamentals, Industrial Techniques, and Applications, Harry E. Martz, Clint M. Logan, Daniel J. Schneberk, Peter J. Shull, CRC Press, May 2016
[6] Schneberk, D., R. Maziuk, B. Soyfer, N. Shashishekhar, and R. Alreja, "Application of Offset-CT Scanning to the Inspection of High Power Feeder Lines and Connections," *AIP Conference Proceedings, Vol. 1706, 26–31 July 2015, Minneapolis, Minnesota, 2016*.